

# Predictions of ultra-harmonic oscillations in coupled arrays of limit cycle oscillators

Alexandra S. Landsman<sup>1</sup>, Ira B. Schwartz<sup>1</sup>

<sup>1</sup>*US Naval Research Laboratory, Code 6792,*

*Nonlinear Systems Dynamics Section,*

*Plasma Physics Division, Washington, DC 20375\**

## Abstract

Coupled distinct arrays of nonlinear oscillators have been shown to have a regime of high frequency, or ultra-harmonic, oscillations that are at multiples of the natural frequency of individual oscillators. The coupled array architectures generate an in-phase high-frequency state by coupling with an array in an anti-phase state. The underlying mechanism for the creation and stability of the ultra-harmonic oscillations is analyzed. A class of inter-array coupling is shown to create a stable, in-phase oscillation having frequency that increases linearly with the number of oscillators, but with an amplitude that stays fairly constant. The analysis of the theory is illustrated by numerical simulation of coupled arrays of Stuart-Landau limit cycle oscillators.

PACS numbers: 05.45.-a, 05.45.Xt

## I. INTRODUCTION

The dynamics occurring in coupled oscillators has been of much interest in both basic and applied science. Since the original early observations of Huygen's of two synchronized coupled nonlinear clocks (See the appendix for a nice description in [1]), theories of coherent motion in limit cycle and phase oscillator arrays having different couplings have become numerous [3, 4, 5, 6]. In most cases studied, however, the arrays are assumed to have a single statistical coupling architecture, such as global coupling [7, 8], nearest neighbor and ring coupling [9, 10], and long range coupling [11], to list just a few.

In many of the examples of coherent motion studied, the synchronized in-phase state and incoherent splay or anti-phase state have both been observed. In coupled semi-conductor lasers, it is known that nature prefers the incoherent states [12], while in Josephson junction arrays which are globally coupled, both in-phase and incoherent states may co-exist [13, 14]. The stability of the in-phase state in most applications has been important in order to maintain frequency control and/or power output in the arrays, such as in coupled lasers and Josephson's junctions.

Recently, interacting arrays of limit cycle oscillators possessing different architectures have been proposed to stabilize a high frequency in-phase state [15]. While numerical simulations exhibit stable in-phase states over a particular range of parameters, no analytical work has been done on the system, and the mechanism behind the onset of stable ultraharmonic oscillations has not been explained. The goal of this paper is to explain the mechanism behind the onset of stable ultraharmonics, obtain analytic results for the critical value of the coupling constant required for this onset, as well as to explore an alternative coupling scheme previously not considered. The paper is organized as follows: In Section II, the equations of motion are introduced and solved exactly, in the absence of global coupling between the two arrays. In Section III, the bifurcation value of the global coupling constant above which stable ultra-harmonic oscillations set in is calculated and shown to depend of frequency, amplitude and total number of oscillators. The physical mechanism behind the onset of stable ultra-harmonics is explained, as resulting from a large constant component in the amplitude-dependent global coupling, that determines the bifurcation value. Above the bifurcation value, the dynamics of one of the arrays become a function of the other, resulting in ultraharmonics. Averaging theory is applied in Section IV to explain the equivalence of

the bifurcation diagrams between the averaged and the full system and to estimate the amplitude of ultraharmonic oscillations. Section V derives an alternative type of coupling that while more complicated in form, has the advantage of creating a higher amplitude ultra-harmonic oscillations, with an amplitude that stays fairly constant as the number of oscillators in the array increases. Section VI concludes and summarizes our results.

## II. BASIC EQUATIONS AND DYNAMICS

The internal dynamics of the uncoupled Stuart-Landau oscillators in normal form is:

$$\dot{\vec{z}} = (\alpha + i\omega)\vec{z} - |\vec{z}|^2\vec{z} \quad (1)$$

where  $\vec{z}$  is a complex variable. The notation used in this paper is similar to that in [15]. Equation (1) can be easily solved by transforming into polar variables, and results in a limit cycle oscillator with frequency equal to  $\omega$  and steady-state amplitude of oscillation equal to  $\sqrt{\alpha}$ . The system considered here consists of two arrays of coupled Stuart-Landau oscillators,  $\{X_j\}$  and  $\{Y_j\}$ , where the index,  $j$  stands for each individual oscillator. Throughout the rest of the paper, the  $\{X_j\}$  and  $\{Y_j\}$  will be referred to simply as  $X$  and  $Y$  arrays. In the absence of coupling, the equations of motion of each oscillator within the arrays is given by Eq. (1). The difference between the two arrays is that  $X$  oscillators possess anti-phase diffusive coupling between oscillators within the array, while the  $Y$  array has in-phase diffusive coupling within the array. The two arrays are globally coupled to each other. The whole system is described by the following set of equations:

$$\dot{\vec{X}}_j = (\alpha_x + i\omega)\vec{X}_j - |\vec{X}_j|^2\vec{X}_j + c_x (X_{j-1} + X_{j+1} - 2X_j) + c_{yx} \sum_{k=1}^N |Y_k| \quad (2)$$

$$\dot{\vec{Y}}_j = (\alpha_y + i\omega)\vec{Y}_j - |\vec{Y}_j|^2\vec{Y}_j + c_y (Y_{j-1} + Y_{j+1} - 2Y_j) + c_{xy} \sum_{k=1}^N |X_k| \quad (3)$$

A schematic diagram of the architecture of the coupled arrays in Eqs. (2) and (3) is shown in Figure (1). In the case of the  $X$  array oscillators, the diffusive coupling between oscillators within the array is out-of-phase, which occurs if  $c_x < 0$ , which we assume. The  $Y$ -array oscillators will all oscillate in-phase in steady-state, which is a direct outcome of the diffusive coupling term,  $c_y > 0$ , so that the in-phase state is the only stable state. From Eqs. (2)

and (3), it is clear that global coupling depends only on the amplitude of oscillators in the two arrays,  $|Y_k|$  and  $|X_k|$ . If this amplitude is approximately conserved, then the main contribution from the global coupling term will be a constant component. In Section V, an alternative coupling scheme that results in a higher oscillatory component in the global coupling, leading to higher intensity ultraharmonics, will be considered.

### Dynamics in the absence of inter-array coupling

In the absence of inter-array coupling,  $c_{xy} = c_{yx} = 0$ , an exact steady-state solution can be obtained for the two arrays. Since in steady-state, all the  $Y$ -array oscillators move in-phase, the diffusive coupling term drops out of the Eq. (3), and the solution reduces to that of a single limit cycle oscillator, so that the index  $j$  on the  $Y$  array will be dropped throughout the rest of the paper. Unlike the  $Y$  array oscillators, the diffusive coupling term in the  $X$  array is negative, so that the oscillators want to be maximally out-of-phase with their nearest neighbors. For a ring of diffusively coupled oscillators, this results in two solutions, depending on whether  $N$  is even or odd:

$$\Delta\phi_{j,j+1}^{even} = \pi \quad (4)$$

$$\Delta\phi_{j,j+1}^{odd} = \pi + \pi/N \quad (5)$$

where  $\Delta\phi_{j,j+1}^{even}$  and  $\Delta\phi_{j,j+1}^{odd}$  is the phase difference between the  $j$ th and the  $j+1$ th oscillator in the  $X$ -array for  $N$ -even and  $N$ -odd, respectively. Since all the oscillators in the  $X$ -array are identical and differ only by a phase-shift, we now have an expression for the steady-state dynamics of  $j+1$  and  $j-1$  oscillators as a function of the  $j$ th oscillator:

$$\vec{X}_{j-1} = e^{-i\Delta\phi_{j,j+1}} X_j \quad \vec{X}_{j+1} = e^{i\Delta\phi_{j,j+1}} X_j \quad (6)$$

Substituting Eq. (6) into Eq. (2), using Eqs. (4) and (5), and setting  $c_{yx} = 0$ , we can now solve for the amplitude of the  $X$ -array oscillators in the absence of global inter-array coupling:

$$A_x^{N-even} = (\alpha_x - 4c_x)^{1/2} \quad (7)$$

for even  $N$ , and

$$A_x^{N-odd} = [\alpha_x - 2c_x (1 + \cos(\pi/N))]^{1/2} \quad (8)$$

for odd  $N$ . The frequency of  $X$  array oscillators is the same as in the  $Y$  array, the limit cycle frequency,  $\omega$ . For  $\alpha_x = \alpha_y$  however, since  $c_x < 0$ , the amplitude of oscillation is higher than that of the in-phase  $Y$ -array, which oscillates at amplitude  $\alpha_y^{1/2}$ . As will be shown in the following section, this difference in amplitude is important to the creation of the stable ultraharmonics and will effect the range of the global coupling constant necessary for stable ultraharmonics, in the case of symmetric coupling.

From Eqs. (4) and (6), it is clear that for  $N$ -even, the  $X$  array splits into two identical subgroups containing  $N/2$  oscillators, where the two subgroups are out-of-phase with each other by  $\pi$ . For  $N$ -odd, the  $X$ -array forms a traveling wave, with phases distributed over the unit circle in increments of  $2\pi/N$ . This can be seen by using Eq. (5), which gives  $2\pi/N$  as the smallest phase difference (between  $j$ th and  $j + 2$ nd oscillators). Since for generation of ultraharmonics at frequency  $N\omega$ , the  $X$  array must form a traveling wave, with phase increments of  $2\pi/N$ , the rest of the paper will focus on  $N$ -odd arrays. The reason why this  $2\pi/N$  distribution of phases is needed for the creation of ultraharmonics at frequency  $N\omega$  will be explained in the following section. Other types of inter-array coupling schemes could be considered that would result in a different phase distribution. For example, global out-of-phase coupling in the  $X$ -array should yield the desired traveling wave distribution for an  $N$ -even, and not just  $N$ -odd arrays.

### III. THE EFFECT OF GLOBAL COUPLING AND CREATION OF STABLE ULTRAHARMONICS VIA A BIFURCATION

It was shown in the previous section that in the absence of global coupling,  $c_{yx} = c_{xy} = 0$ , the steady state dynamics of the two arrays are that of a simple harmonic oscillator, with amplitudes given by  $\alpha_y^{1/2}$  and Eq. (8), for the  $Y$  and  $X$  arrays, respectively. Since the global coupling term is a function of amplitude only (see Eqs. (2) and (3)), we would expect the global coupling to introduce a constant component into Eqs. (2) and (3). In fact, if the coupling is one-way, that is if we set  $c_{yx} = 0$ , then the global coupling term only contributes a constant component and no ultraharmonics can occur in the  $Y$  array. This explains the previously made observation [15] that mutual coupling between the two arrays is required to induce ultraharmonic oscillations. It follows that the global coupling term in the  $X$  array must create a perturbation in the amplitude of the  $X$  oscillators, so that it is no longer

a conserved quantity. To understand how this happens, we examine the weakly coupled case,  $c_{yx}, c_{xy} \ll 1/(\alpha_{x,y}^{1/2}N)$ . Then, in the absence of resonant interactions, the steady-state dynamics of the two arrays is given to lowest order by:

$$\dot{\vec{X}}_j = (\tilde{\alpha}_x + i\omega)\vec{X}_j - |\vec{X}_j|^2\vec{X}_j + C_y \quad (9)$$

$$\dot{\vec{Y}} = (\alpha_y + i\omega)\vec{Y} - |\vec{Y}|^2\vec{Y} + C_x \quad (10)$$

where  $\tilde{\alpha}_x = \alpha_x - 2c_x(1 + \cos(\pi/N))$ . The index  $j$  has been dropped in the  $Y$  array, since the array oscillates in-phase in steady-state. The subscript on  $C_y$  ( $C_x$ ) indicates that the term comes from the global coupling from the  $Y$  to the  $X$  array (from the  $X$  to the  $Y$  array). The constant components  $C_x$  and  $C_y$  in Eqs. (9) and (10) are given by:

$$C_y = c_{xy}N\alpha_y^{1/2}; \quad C_x = c_{xy}N[\alpha_x - 2c_x(1 + \cos(\pi/N))]^{1/2}. \quad (11)$$

Since  $c_x < 0$ ,  $C_x > C_y$ , it is clear that the  $X$  array has a stronger effect on the dynamics of the  $Y$  array than vice versa, even in the case of symmetric coupling:  $c_{xy} = c_{yx}$ . Equations of the form (9) and (10) have been studied previously in connection with forced Van der Pohl oscillators [2]. The main characteristic of these equations is that they execute a limit cycle below a certain critical value of the constants,  $C_y, C_x$ . Above the critical bifurcation value, the oscillations are damped out, so that the system reaches a stable equilibrium (a sink). There is also a narrow intermediate range (between the limit cycle and the sink region) which will not be discussed, but for a more detailed description see [2]. Equation (9) can be used to understand how ultraharmonic oscillations are created in the coupling term,  $c_{xy} \sum_{k=1}^N |X_k|$  in Eq. (3). The constant component,  $C_y$ , of the global coupling in Eq. (9), breaks the symmetry about the origin, making the amplitude of oscillation dependent on the phase of the oscillator. In phase-space, this corresponds to the shifting of the center of limit cycle from the origin. Now, all of the oscillators in the  $X$  array have amplitudes which oscillate at the frequency of the limit cycle,  $\omega$ . Since the phases of the oscillators in the  $X$  array are distributed in increments of  $2\pi/N$ , there are  $N$  peaks in amplitude over a single limit cycle oscillation. Adding all of the amplitudes together in the coupling term,  $c_{xy} \sum_{k=1}^N |X_k|$  creates an ultraharmonic oscillation at frequency  $N\omega$ . It follows that the global coupling term in the  $Y$  array will have a component oscillating at an ultraharmonic frequency,  $N\omega$

as well as a much larger constant component,  $C_x$ . If this constant component,  $C_x$ , is above the bifurcation value,  $C_x > C_{bx}$ , the  $Y$  array will be driven into the steady-state region of phase-space. It will then execute ultraharmonic oscillations with frequency  $N\omega$  about that steady state. This can be better explained using averaging theory that applies when the system, given by Eq. (10) is close to steady-state (when  $C_x > C_{bx}$ ) and will be explored in the following section.

The bifurcation values  $C_{bx}$  and  $C_{by}$  for  $C_x$  and  $C_y$ , respectively, occur when the the real part of the nullcline straightens out, leading to a single equilibrium, which is a steady state. Calculating the bifurcation value for Eqs. (9) and (10),

$$C_b = 2 \left( \frac{\tilde{\alpha}}{3} \right)^{3/2} + \left( \frac{3}{16\tilde{\alpha}} \right)^{1/2} \omega^2 \quad (12)$$

where  $\tilde{\alpha} = \alpha_y$  for  $C_{bx}$  and  $\tilde{\alpha} = \alpha_x - 2c_x(1 + \cos(\pi/N))$  for  $C_{by}$ . For  $\tilde{\alpha}/\omega \geq 1$ ,  $C_b$  is a monotonically increasing function of  $\tilde{\alpha}$ , so that the critical bifurcation for the  $X$  array is higher then for the  $Y$  array (for  $\alpha_x = \alpha_y$ ), since  $c_x < 0$ . We are now in a position to give an explanation of the mechanism behind the onset of ultraharmonic oscillations in the  $Y$  array. As the symmetric global coupling constant,  $c_{xy} = c_{yx}$ , increases, a critical bifurcation value is reached in the constant component of the global coupling, whereby the  $Y$  array undergoes a bifurcation into a sink region of the phase-space, while the  $X$  array is still executing a limit cycle oscillation. After undergoing a bifurcation, the  $Y$  array oscillators are driven by the oscillatory ultraharmonic component of the coupling from the  $X$ -array and execute ultraharmonic oscillations about a steady state, which is determined by the constant component,  $C_x$ .

The constant component,  $C_x$ , of the coupling term  $c_{xy} \sum_{k=1}^N |X_k|$  in Eq. (3) is given by

$$C_x = c_{xy} N \bar{A}_x \quad (13)$$

where  $\bar{A}_x$  is the average amplitude of the  $X$  array. If the amplitude of the  $X$  array is not substantially affected by the global coupling term, then  $\bar{A}_x$  can be approximated by Eq. (8). Substituting  $C_{bx}$  from Eq. (12) and  $A_x$  from Eq. (8) into Eq. (13) and solving for  $c_{xy}$ , we get an approximation of the bifurcation value of the global coupling constant for the onset of stable ultraharmonic oscillations,

$$c_{xy}^b = \frac{2(\alpha_y/3)^{3/2} + (3/16\alpha_y)^{1/2} \omega^2}{N[\alpha_x - 2c_x(1 + \cos(\pi/N))]^{1/2}} \quad (14)$$

Figure (2) plots the bifurcation values of the global coupling constant, given by Eq. (14) as a function of the diffusive coupling in the  $X$  array,  $c_x$ . Note the excellent agreement between the analytically derived curve and the numerical simulation. The slight consistent under-estimate of  $c_{xy}^b$  comes from using the unperturbed amplitude,  $A_x$ , as given by Eq. (8). As can be seen from the figure, however, the unperturbed amplitude,  $A_x$  is an excellent approximation for the globally coupled system over a whole range of values. The bifurcation values,  $c_{xy}^b$  given by Eq. (14) also agree closely with the numerically calculated values [15]. Thus substituting  $N = 3$ ,  $\alpha_x = \alpha_y = 1$ ,  $\omega = 1/2$  and  $c_x = -0.4$  into Eq. (14), we get the bifurcation value of  $c_{xy}^b = .1108$ . This is the value where all unstable solutions disappear, and only stable equilibrium solution exists. Compare this to the corresponding value of  $c_{xy}^b = .1123$  found numerically.

Figure (3) plots the bifurcation values of the global coupling constant, given by Eq. (14) as a function of the parameter,  $\alpha_x$ . Higher values of  $\alpha_x$ , relative to  $\alpha_y$  lead to higher relative amplitude of oscillation of the  $X$  array, resulting in a lower bifurcation value of  $c_{xy}^b$  and a greater range of the global coupling constant,  $c_{xy}^b$  for generation of ultraharmonics. From Eq. (14), for large values of the diffusive coupling,  $c_x$ , the bifurcation value for the onset of ultraharmonic oscillations decreases as  $1/\sqrt{|c_x|}$ . Since Eq. (12) is a monotonically increasing function of  $\tilde{\alpha}$ , it is clear that the bifurcation value of the  $X$  array into a sink increases as a function of  $|c_x|$ . It follows that as  $|c_x|$  increases, the range of the coupling constant  $c_{xy} = c_{yx}$  whereby stable ultraharmonics are induced in the  $Y$ -array also increases. If the value of the global coupling is too high, then the  $X$  array undergoes a bifurcation, resulting in oscillation death. So, the coupling constant should be high enough,  $c_{xy} > c_{xy}^b$  so that the dynamics in Eq. (10) bifurcate from limit cycle into a sink, but low enough so that the oscillators in the  $X$  array undergo a limit cycle oscillation at the natural frequency,  $\omega$ .

#### IV. AVERAGING THEORY AND THE CREATION OF ULTRAHARMONIC OSCILLATIONS

The mechanism behind the onset of ultraharmonics has been explained in the previous section. For small amplitude ultraharmonics, averaging theory can be used to prove that the frequency of these oscillations is the multiple of the limit-cycle frequency,  $N\omega$ . Averaging is



applicable to the systems of the form

$$\dot{x} = \epsilon f(x, t), \quad x \in \mathcal{R}^n \quad (15)$$

where  $\epsilon$  is small and  $f$  is,  $T$ -periodic in  $t$  [2]. In our case, the periodic forcing comes from the ultraharmonic frequency,  $N\omega$ , in the periodic coupling term  $c_{xy} \sum_{k=1}^N |X_k|$ . In system of the form given by Eq. (15), the relatively high frequency of periodic forcing constrasts with the slow evolution of the averaged system. Thus the averaging theory can be applied if the amplitude of ultraharmonic oscillations about the equilibrium given by solving Eq. (10) is small. As previously explained, the global coupling term can be broken up into a large constant component,  $C_x$ , and the relatively small oscillatory component,  $\tilde{C}_x$ :

$$c_{xy} \sum_{k=1}^N |X_k| = C_x + \tilde{C}_x(t) \quad (16)$$

where  $\tilde{C}_x \ll C_x$ . Dividing Eq. (3) by  $C_x$ , we can now rewrite it as

$$\dot{\bar{Y}} = F(\bar{Y}) + \tilde{C}_x(t)/C_x \quad (17)$$

where variable  $\bar{Y}$  has been rescaled, and  $F(\bar{Y})$  is the right-hand side of Eq. (10), scaled by  $C_x$ . Near the equilibrium solution of Eq. (10), Eq. (17) has the same form as Eq. (15), since both  $\tilde{C}_x(t)/C_x$  and  $F(\bar{Y})$  are small. Applying the Averaging Theorem (see for example [2]), we can thus solve for  $Y$ ,

$$Y = \bar{Y} + W \quad (18)$$

where  $\bar{Y}$  is the solution of the averaged system, given by Eqs. (10), and  $W$  is given by:

$$\frac{\partial W}{\partial t} = \tilde{C}_x \quad (19)$$

Approximating  $\tilde{C}_x$  to lowest order as a sinusoidal function at frequency  $N\omega$ , we get an expression for  $Y$  as a function of  $\tilde{C}_x$ ,

$$Y \approx \bar{Y} + \frac{\tilde{C}_x}{N\omega} \quad (20)$$

Figure (4) compares numerically calculated amplitude of  $Y$  oscillation to the one given by Eq. (20),  $\tilde{C}_x/N\omega$ . The agreement is better at lower ultraharmonic amplitudes, in accordance to the assumptions under which Eq. (20) was derived:  $\tilde{C}_x(t)/C_x \ll 1$ .

As can be seen from Eq. (20), the amplitude of ultraharmonic oscillations is inversely proportional to the ultraharmonic frequency,  $N\omega$ . We thus expect a degradation of amplitude as the number of oscillators in the array increases. The next section proposes a different coupling term that both achieves a higher amplitude of ultraharmonic oscillations, and does not suffer degradation in amplitude as  $N$  increases.

## V. COUPLING FOR ACHIEVING HIGH FREQUENCY CONSTANT AMPLITUDE OSCILLATIONS

Up to this point, we have focused on amplitude dependent global coupling, of the form given by Eqs. (2) and (3). For this form of coupling, the amplitude of ultra-harmonic oscillations is low and falls as  $N$  increases. The amplitude of ultraharmonics cannot be significantly increased by increasing the mutual coupling strength, since high mutual coupling leads to a bifurcation of the  $X$  array and oscillator death. From the previous sections, it should be clear that any form of coupling, which is a periodic function of some frequency,  $\omega_f$ , induces oscillations at that frequency (for sufficiently low amplitude) as long as the constant part of the coupling,  $C_x$ , is above the bifurcation value:  $C_x > C_{bx}$ . It should therefore be possible to better control the amplitude of ultra-harmonic oscillations and even the frequency by the choice of the coupling function. In this section, a form of coupling is derived that induces ultraharmonic oscillations in the  $Y$  array at frequency  $2\omega N$  (rather than  $\omega N$ ), with an amplitude that stays relatively constant as  $N$  increases.  $N$  used will be odd, since as previously discussed, only  $N$  odd arrays have phases in increments of  $2\pi/N$  in the presence of diffusive coupling.

As shown in Section II, in the absence of inter-array coupling,  $c_{yx} = 0$ , the  $X$  array oscillates as a collection of simple harmonic oscillators, at an amplitude given by Eq. (8), and with a phase difference of  $\pi + \pi/N$  between nearest neighbors and  $2\pi/N$  jumping over a neighbor. The function describing each oscillator in a steady-state is given by:

$$X_{jr} = A_x \cos(\omega t - \phi_j) \quad (21)$$

where  $X_{jr}$  denotes the real part of the  $j$ th oscillator,  $\vec{X}_j$ , and  $A_x$  is the amplitude given by Eq. (8). The phase,  $\phi_j$  is given by

$$\phi_j = (j - 1) (\pi + \pi/N) \quad (22)$$

where Eq. (5) was used. Since  $\{X_{jr}\}$  is a collection of sinusoidal functions with phases distributed in equal increments over the interval  $[0, 2\pi]$ , an ultra-harmonic coupling function,  $c_{xy} \sum_{k=j}^N g(X_j)$ , can thus be created by simply summing the real part of the oscillation,  $c_{xy} \sum_{k=1}^N g(X_j) = \sum_{j=1}^N |X_{jr}|$ . In this case however, the constant component of the coupling,  $C_x$  increases substantially as  $N$  increases, and the relative amplitude of the ultra-harmonic component,  $\tilde{C}_x$  drops substantially with  $N$  (where  $\sum_{j=1}^N |X_{jr}| = C_x + \tilde{C}_x$ ). Figure 5 shows this effect for  $N = 3$  and  $N = 5$ . It is possible to increase the amplitude of the oscillatory component of the coupling and decrease  $C_x$  by taking the sum of some power of  $X_{jr}$ ,

$$c_{xy} \sum_{j=1}^N g(X_j) = c_{xy} N \sum_{j=1}^N |\tilde{X}_{jr}|^n \quad (23)$$

where  $n$  is an integer yet to be determined, and  $\tilde{X}_{jr}$  has been normalized (divided by  $A_x$ ):

$$\tilde{X}_{jr} = \cos(\omega t - \phi_j) \quad (24)$$

where  $\phi_j$  is given by Eq. (22). The factor of  $N$  multiplying Eq. (23) is there to compensate for the fall of ultraharmonic amplitude as the frequency increases (see Section IV). We need to find an expression for  $n$  as a function of  $N$  and  $C_x$ ,  $n(N, C_x)$ , such that the amplitude of oscillation stays fairly constant as  $N$  increases.

From Eq. (24), it is clear that increasing  $n$  (for even  $n$ ) in Eq. (23) will lead to sharper, more narrow peaks centered around  $\omega t - \{\phi_j\} = 0, \pi$ , with  $j$  running between 1 and  $N$ . Thus with increasing  $n$ , there will be less overlap between neighboring peaks in Eq. (24), leading to a lower value of  $C_x$ , the constant component of the coupling. (see Figure 6). In the limit as  $n \rightarrow \infty$ , the sum in Eq. (23) becomes, as a function of  $t$ ,

$$c_{xy} \sum_{k=1}^N |\tilde{X}_{kr}|^n = c_{xy} \int_{t+1/n}^{t-1/n} \delta(\sin[2N\omega\tilde{t} - \phi_1]) d\tilde{t} \quad (25)$$

where  $\delta$  is the delta function, and  $\phi_1$  is the initial phase of the first oscillator. In other words, the normalized coupling from the  $X$  array as  $n \rightarrow \infty$  is given by a series of spikes, occurring at frequency  $2n\omega$  and of amplitude  $c_{xy}$ . Figure 6 shows  $\sum_{k=1}^N |\tilde{X}_{kr}|^n$  for  $n = 60$ . We can already see sharply defined spikes that approach a sum of spikes of a unit amplitude as  $n \rightarrow \infty$ . Eq. (25) has frequency of  $2N\omega$  rather than  $N\omega$ , the frequency generated when the amplitudes are added. This happens because each  $|X_{kr}|^n$  has 2 spikes over the time

interval  $[0, 2\pi/\omega]$ , so that summing over  $N$  oscillators leads to a waveform of frequency  $2\omega N$ , rather than  $\omega N$ , as for amplitude coupled arrays (see Figure 7). Since neighboring peaks are separated by  $\pi/N$ , the two nearest spikes intersect at a phase difference of  $\pi/2N$  from the top of each peak. Assuming that the exponent,  $n$ , is sufficiently large so that only nearest neighboring spikes have significant overlap (see Fig. 6), we are led to the following equation for the constant component of the coupling from the  $X$ -array to the  $Y$ -array:

$$C_x = 2N \cdot c_{xy} [\cos(\pi/2N)]^n, \quad (26)$$

where the exponent,  $n$  is a function of  $N$ , such that  $\cos(\pi/2N)$  stays constant as  $N$  increases. Therefore  $C_x$  increases linearly with  $N$ , a situation similar to the amplitude coupled arrays, where the constant component of the coupling also increases linearly as  $N$ , for large  $N$  (see Eq. (13)). The amplitude of the oscillatory component of the coupling is found by subtracting the constant component,  $C_x$ , given by Eq. (26) from the peak of the normalized oscillation, which occurs at one,

$$\max(\tilde{C}_x) = c_{xy} N (1 - 2[\cos(\pi/2N)]^n). \quad (27)$$

Thus, unlike amplitude coupled arrays, the oscillatory component of the coupling also increases linearly with  $N$ , which prevents the degradation of amplitude seen in the amplitude coupled case. Using Eq. (20) with  $2N\omega$  in the denominator (since that is the frequency of the drive), the amplitude of ultraharmonic oscillations can be approximated as

$$A_y \approx \frac{c_{xy}}{2\omega} (1 - 2[\cos(\pi/2N)]^n) \quad (28)$$

and should therefore stay fairly constant as  $N$  increases if  $[\cos(\pi/2N)]^n \sim \text{const}$  for large  $N$ . For large  $N$ , we can approximate the cosine term as

$$\cos(\pi/2N) \approx 1 - (\pi/2N)^2 \approx \exp\left(-\frac{\pi^2}{2N^2}\right) \quad (29)$$

where the first approximation came from taking the first two terms of a series expansion of a cosine function and the second approximation came from expanding the exponential in a series, taking the first two terms and comparing them to  $1 - (\pi/2N)^2$ . Thus in order for  $A_y$  in Eq. (28) to stay fairly constant as  $N$  increases, for  $N$  large, we need  $n \propto N^2$ . When taking the power,  $n$  should be rounded to the nearest even number. Choosing

$$n = KN^2 - KN^2 \text{ mod } 2 \quad \text{if} \quad KN^2 \text{ mod } 2 \leq 1 \quad (30)$$

$$n = KN^2 - KN^2 \bmod 2 + 2 \quad \text{if} \quad KN^2 \bmod 2 > 1. \quad (31)$$

The above equations ensure that  $n$  is rounded to the nearest even number.  $K$  is some constant, which can be chosen to achieve a desired value of  $C_x$  (for example  $K = 2/3$  is a good choice). Using Eqs. (28)-(31) we obtain an approximate expression for the amplitude of ultraharmonic oscillations when  $N$  is large:

$$A_y \approx \frac{c_{xy}}{2\omega} \left( 1 - 2 \exp \left( -\frac{\pi^2 K}{2} \right) \right). \quad (32)$$

From the above equation, the coupling strength,  $c_{xy}$  and  $K$  can be chosen to obtain the desired amplitude of ultraharmonics, with a maximum possible amplitude being  $A_y \approx c_{xy}/2\omega$ .

Figure (8) shows the amplitude of ultraharmonics,  $A_y$ , as a function of  $N$  for both the drive coupling given in Eq. (23), with  $n$  given by Eqs. (30) and (31) and mutual coupling analyzed in the previous section. The parameters were chosen such that the constant component of the coupling,  $C_x$  is the same in both cases. The solid line for the drive dependent coupling is the result of connecting the data points for the odd  $N$  values between  $N = 3$  and  $N = 31$ . The amplitude of ultraharmonics asymptotes to a constant value of around 0.033, close to the value predicted by using Eq. (32) of around 0.028. It is clear that the amplitude of ultraharmonics generated by the drive is significantly higher than that by the mutual coupling, given by Eqs. (2) and (3). In addition, the drive coupling does not suffer from oscillator death, thus the amplitude will stay constant while  $N$  increases. In contrast, increasing  $N$  for mutual coupling leads to oscillator death, unless the coupling constants  $c_{xy}, c_{yx}$  are also decreased (leading to an even further fall in amplitude). In Figure (8), oscillator death occurs at just  $N = 9$ , for the coupling used. Thus the drive has many advantages, such as a relatively high, easily controllable amplitude that does not degrade with an increase in  $N$  and does not suffer from oscillator death, which occurs in mutually coupled arrays. However, since  $n$  increases as  $N^2$ , high ultraharmonics,  $N\omega$ , require rather high powers in the coupling function.

## VI. CONCLUSION

The mechanism behind the generation of ultra-harmonic oscillations in two mutually coupled arrays of limit cycle oscillators was analyzed. These ultra-harmonic oscillations were shown to occur as a result of a bifurcation that results when the coupling from the  $X$  to the  $Y$

array exceeds a certain value. This coupling consists of a large constant component, since the coupling is amplitude-dependent, and a smaller ultraharmonic oscillatory component that results from the breaking of symmetry in the  $X$ -array due to coupling from the  $Y$ -array. This smaller oscillatory component of the coupling induces the  $Y$  array to oscillate at an ultraharmonic frequency around the equilibrium determined by the large constant component of the coupling. It was also shown that in the case of amplitude-dependent coupling, the ultraharmonic oscillation is the result of a mutual interaction between the two arrays (rather than a master-slave system), since the coupling from the  $Y$  to the  $X$  array is necessary to induce an oscillation in the otherwise conserved amplitude of  $X$  oscillators.

The range of inter-array coupling constants whereby ultra-harmonic oscillations are produced was derived for symmetric  $c_{xy} = c_{yx}$  coupling, but can be generalized to non-symmetric coupling, where  $c_{xy} \neq c_{yx}$ . For symmetric coupling, this range depends on the limit cycle frequency, the amplitude of oscillation and the strength of nearest-neighbor coupling within the  $X$  array. The allowable range of inter-array coupling constant increases with an increase in strength of the diffusive coupling,  $c_x$ , in the out-of-phase coupled  $X$  array. Thus higher absolute values of  $c_x$  lead to a greater possible range of values of the inter-array coupling constant whereby ultra-harmonic oscillations are created. The  $Y$  array diffusive coupling strength,  $c_y$ , on the other hand, does not affect the conditions for creation of stable ultraharmonics, since the diffusive coupling term drops out in steady-state for in-phase coupled arrays. The derived bifurcation values for the inter-array coupling constant agree well with numerical simulation, and can be used to tune the value of the coupling constant to control the amplitude of the ultra-harmonic oscillations.

For achieving better-controlled, higher amplitude ultra-harmonic oscillations, another form of coupling was suggested. This one-way coupling has the advantage of achieving higher amplitude ultra-harmonic oscillations that do not fall in amplitude as the number of oscillators, and therefore the ultra-harmonic frequency, increases. It also does not suffer from oscillator death, which puts an upper limit on the strength of symmetric coupling that can be used in amplitude coupled arrays. The suggested form of coupling, however, requires increasingly more complicated forms of the coupling function as  $N$  increases and may be more difficult to implement experimentally.

Finally, though the methods of analysis here were applied to oscillator of Stuart-Landau type, they may be applied to various applications of interest, where both frequency and

power control are required. Such examples of the stabilization of in-phase arrays occur in such areas as electronic circuits for radar [18], phase locked nano-scale magnets used for microwave sources [19], power systems [20], and Josephson junction arrays used for terahertz sources [21].

## ACKNOWLEDGEMENTS

This work was supported by a grant from the Office of Naval Research. ASL is currently a post doctoral fellow with the National Research Council.

---

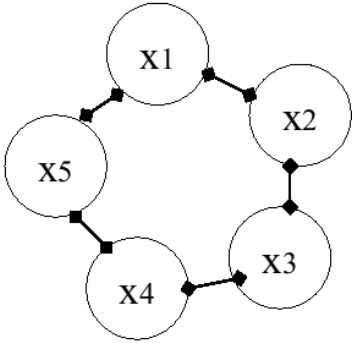
\* Electronic address: jalandasma@cantor.nrl.navy.mil

- [1] A. Pikovsky, M. Rosenblum, and J. Kurths, *Synchronization: A universal concept in nonlinear science* (Cambridge University Press, Cambridge, 2001).
- [2] J. Guckenheimer, and P. Holmes, *Nonlinear Oscillations, Dynamical Systems and Bifurcations of Vector Fields* (Springer-Verlag, New York, 1983).
- [3] H. Daido, *Progress Of Theoretical Physics* **88**, 1213 (1992).
- [4] H. Daido, *Progress Of Theoretical Physics* **89**, 929 (1993).
- [5] Y. Kuramoto and I. Nishikawa, *Journal Of Statistical Physics* **49**, 569 (1987).
- [6] S. H. Strogatz, *Physica D* **143**, 1 (2000).
- [7] A. Pikovsky, O. Popovych, and Y. Maistrenko, *Physical Review Letters* **8704** (2001).
- [8] J. Teramae and Y. Kuramoto, *Physical Review E* **6303** (2001).
- [9] P. L. Buono, M. Golubitsky, and A. Palacios, *Physica D* **143**, 74 (2000).
- [10] H. F. El-Nashar, Y. Zhang, H. A. Cerdeira, and F. Ibiyinka, *Chaos* **13**, 1216 (2003).
- [11] M. Marodi, F. d'Ovidio, and T. Vicsek, *Physical Review E* **66** (2002).
- [12] H. G. Winful and S. S. Wang, *Applied Physics Letters* **53**, 1894 (1988).
- [13] I. B. Schwartz and K. Y. Tsang, *Physical Review Letters* **73**, 2797 (1994).
- [14] K. Y. Tsang and I. B. Schwartz, *Physical Review Letters* **68**, 2265 (1992).
- [15] A. Palacios, R. Carretero-Gonzalez, P. Longhini, N. Renz, V. In, A. Kho, J. D. Neff, B. K. Meadows, and A. R. Bulsara, *Physical Review E* **72** (2005).
- [16] M. Golubitsky, M. Pivato, and I. Stewart, *Dynamical Systems-An International Journal* **19**,

- 389 (2004).
- [17] D. Armbruster and P. Chossat, *Physics Letters A* **254**, 269 (1999).
- [18] V. In, A. Kho, J. D. Neff, A. Palacios, P. Longhini, and B. K. Meadows, *Physical Review Letters* **91** (2003).
- [19] F. B. Mancoff, N. D. Rizzo, B. N. Engel, and S. Tehrani, *Nature* **437**, 393 (2005).
- [20] E. H. Abed and P. P. Varaiya, *International Journal Of Electrical Power & Energy Systems* **6**, 37 (1984).
- [21] D. G. Aronson, M. Golubitsky, and M. Krupa, *Nonlinearity* **4**, 861 (1991).



**$\{X_j\}$ : Out-of-phase  
diffusive coupling**



**global all-to-all  
inter-array coupling**



**$N=5$**

**$\{Y_j\}$ : In-phase  
diffusive coupling**

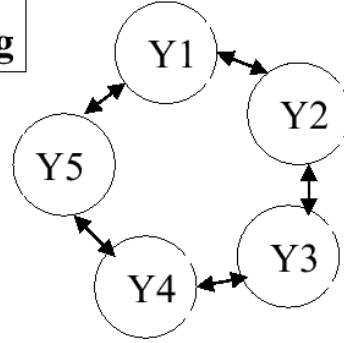


FIG. 1: Two diffusively coupled arrays coupled to each other via global coupling, for  $N = 5$ . The  $X$  array has out-of-phase diffusive coupling, and the  $Y$  array has in-phase diffusive coupling. The two arrays are globally coupled to each other.

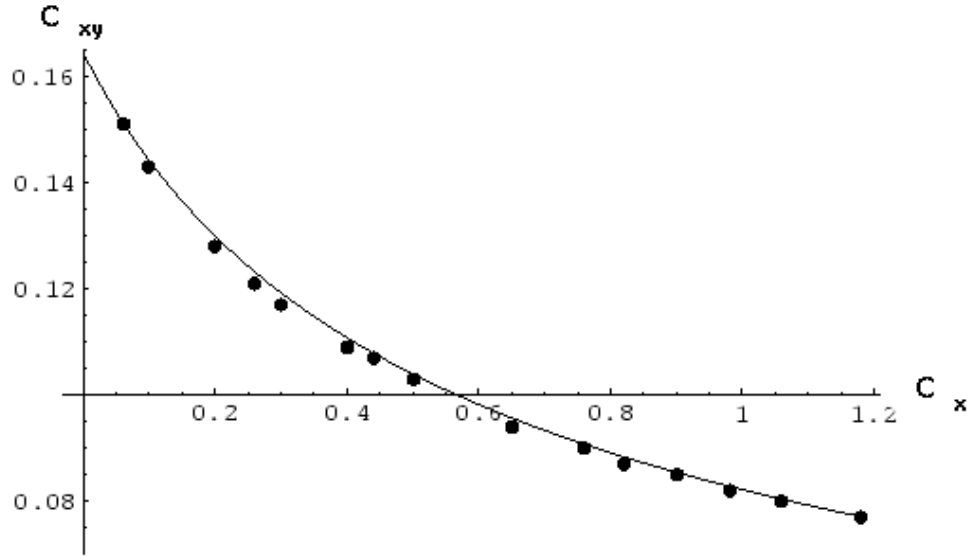


FIG. 2: Bifurcation values of the global coupling constant,  $c_{xy}$  as a function of out-of-phase diffusive coupling,  $c_x$ . The solid line is a plot of the analytically derived Eq. (14). The numerical values are also shown on the graph

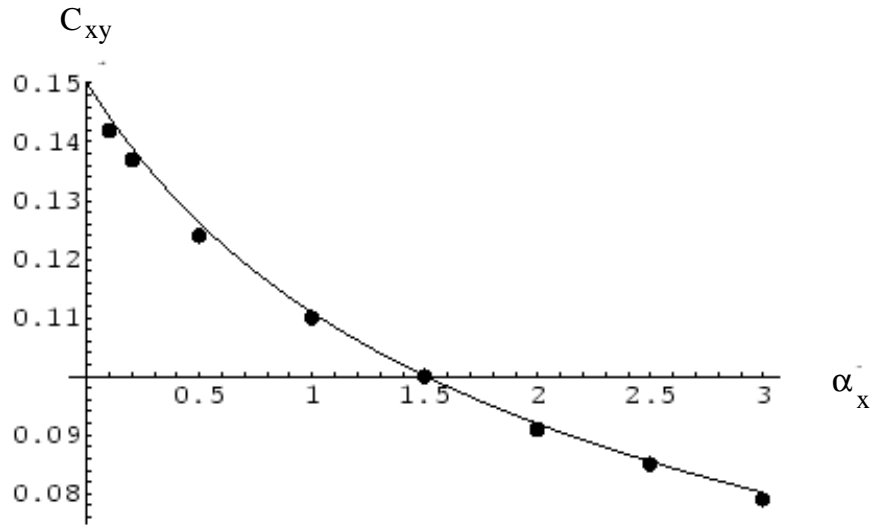


FIG. 3: Bifurcation values of the global coupling constant,  $c_{xy}^b$  as a function of amplitude,  $\alpha_x$ . Both the analytically derived dependence and the numerics are shown

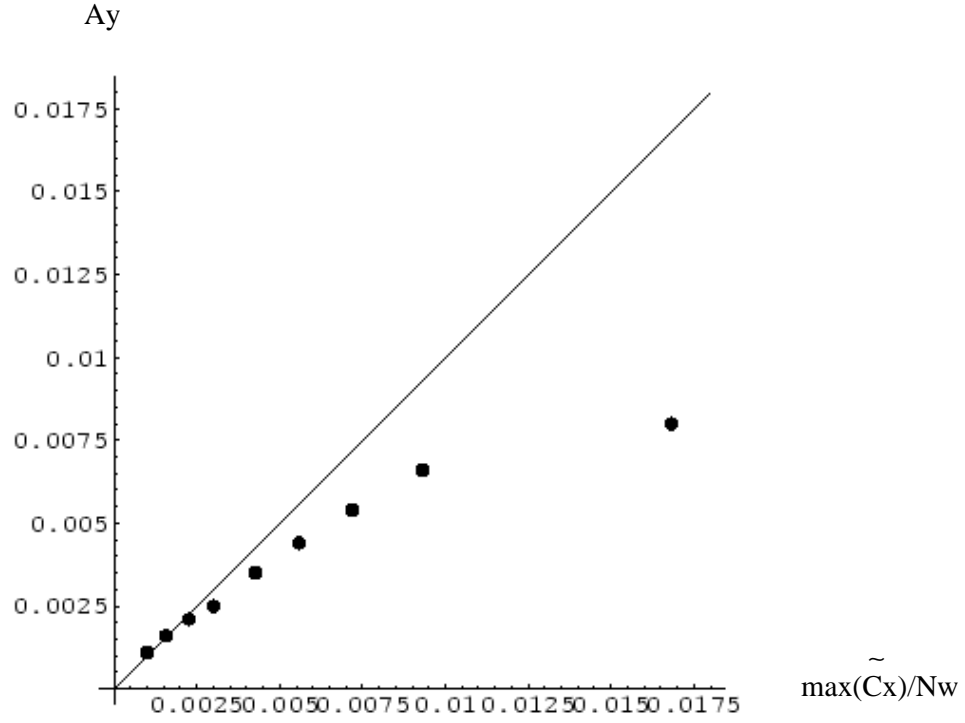


FIG. 4: Amplitude of ultraharmonic oscillations,  $A_y$  vs.  $\max(\tilde{C}_x)/N\omega$ . At lower amplitudes, the oscillations fall on the  $A_y = \max(\tilde{C}_x)/N\omega$  line, in accordance with Eq. (20).

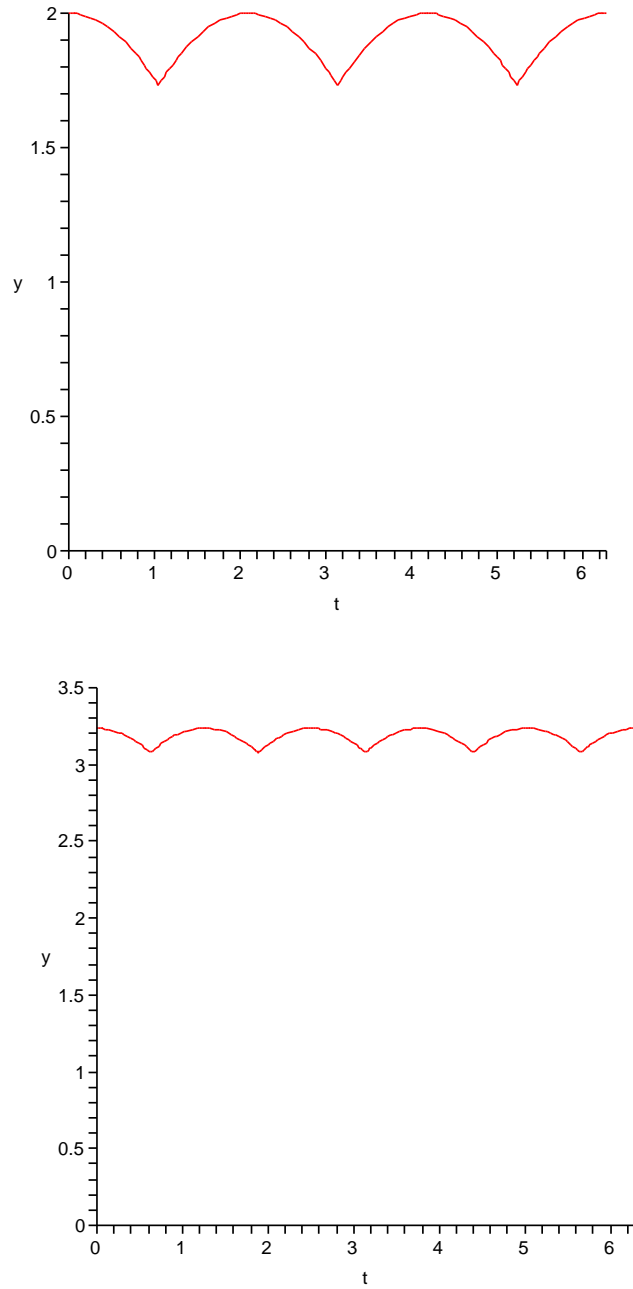


FIG. 5: Top:  $\sum_{j=1}^N |X_{jr}|$  for  $N = 3$ . Bottom:  $\sum_{j=1}^N |X_{jr}|$  for  $N = 5$ . In both cases  $\alpha = 1$ ,  $\omega = 1/2$ ,  $c_{yx} = 0$ . As  $N$  increases, the constant component for this form of coupling increases, while the relative value of the oscillatory component falls.

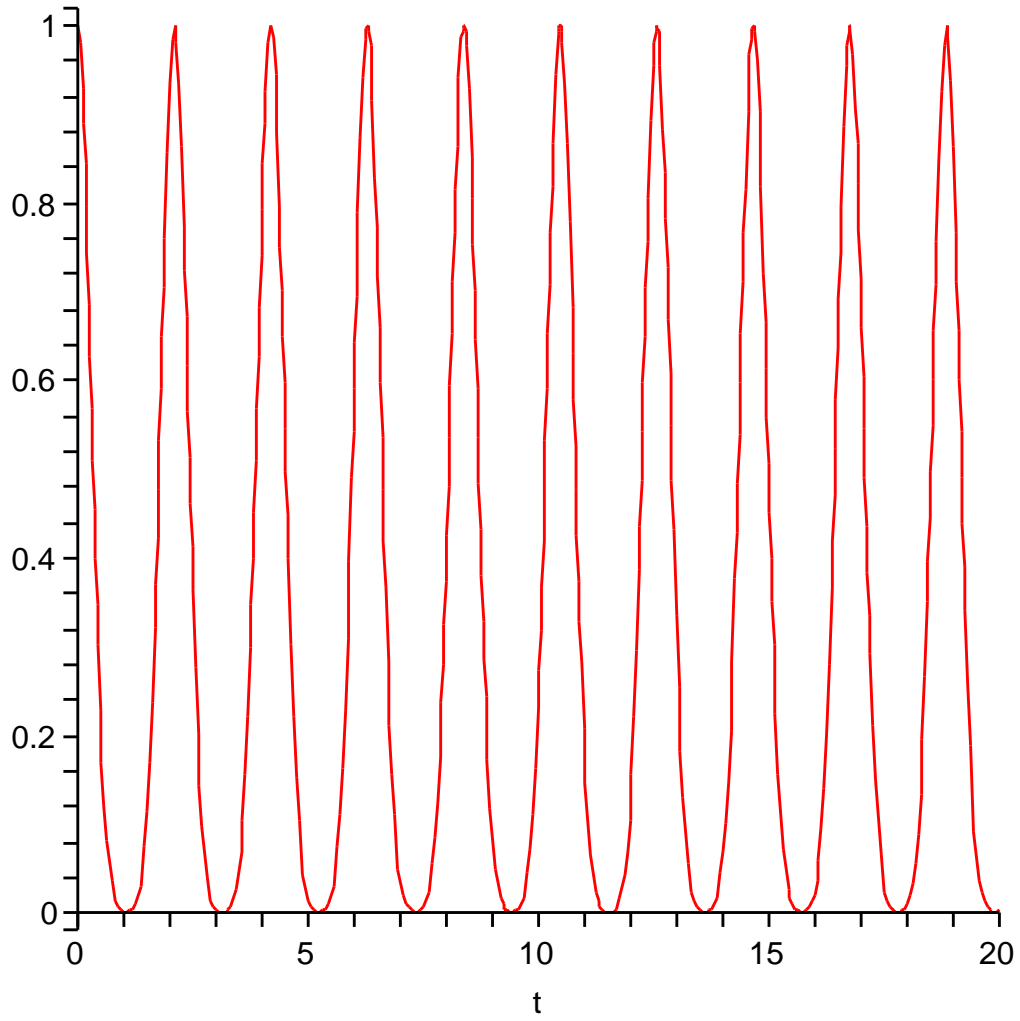


FIG. 6: Drive given by Eq. (23) for high  $n$  ( $n = 60$ ). The peaks narrow substantially, with less overlap between neighboring peaks as  $n$  increases.

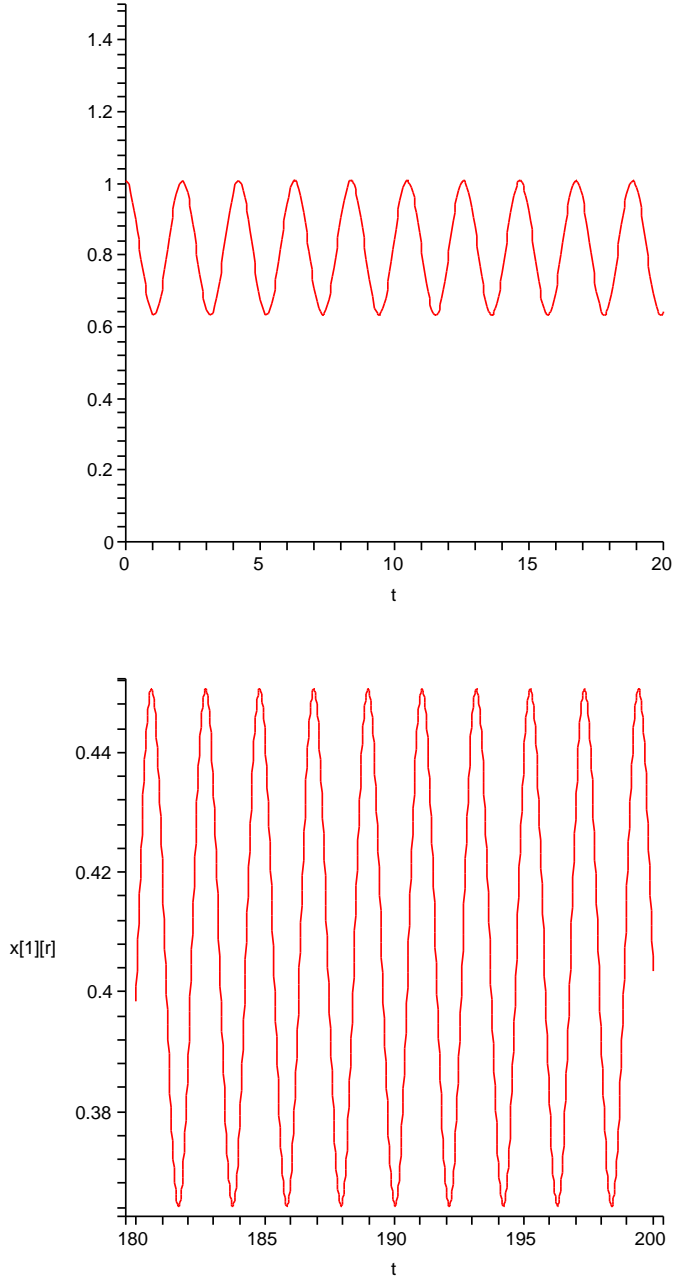


FIG. 7: Oscillations with coupling given by Eq. (23). Top: the coupling term,  $c_{xy}N \sum_{j=1}^N |\tilde{X}_{jr}|^n$ , with  $C_x = 0.8$  and  $\tilde{C}_x = 0.8$ . Bottom: The ultraharmonic oscillations induced in the  $Y$  array by the coupling shown at the top.  $\alpha = 1$ ,  $\omega = 1/2$ ,  $c_{xy} = 0.36$ ,  $c_{yx} = 0$ ,  $N = 3$ .

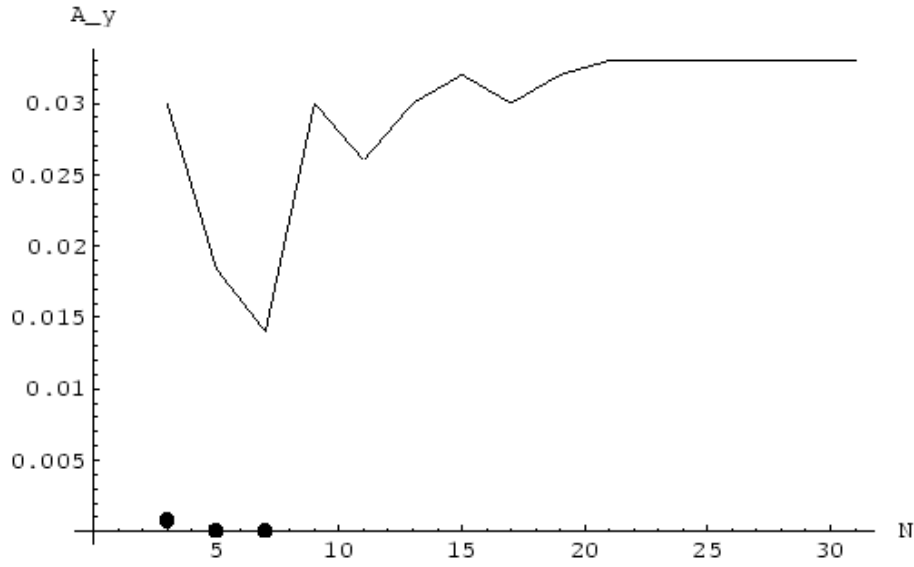


FIG. 8: Solid line: numerically found amplitude of ultraharmonic oscillation,  $A_y$ , with the drive coupling, as a function of  $N$ ,  $K = 2/3$ . Data points: corresponding amplitude of ultraharmonics with the standard amplitude coupling. The constant part of the coupling,  $C_x$  is the same for both cases,  $c_{xy} = c_{yx} = .1134$ ,  $\alpha_x = \alpha_y = 1$ ,  $\omega = 1/2$